Chinese Chemical Letters 36 (2025) 109596

Contents lists available at ScienceDirect

Chinese Chemical Letters

journal homepage: www.elsevier.com/locate/cclet

B-embedded narrowband pure near-infrared (NIR) phosphorescent iridium(III) complexes and solution-processed OLED application

Fuzheng Zhang[a], Chao Shi[a,*], Jiale Li[b], Fulin Jia[a], Xinyu Liu[a], Feiyang Li[a], Xinyu Bai[a], Qiuxia Li[a,*], Aihua Yuan[a], Guohua Xie[b,*]

[a] School of Environmental and Chemical Engineering, Jiangsu University of Science and Technology, Zhenjiang 212003, China
[b] The Institute of Flexible Electronics (Future Technologies), Xiamen University, Xiamen 361005, China

ARTICLE INFO

Article history:
Received 22 December 2023
Revised 15 January 2024
Accepted 29 January 2024
Available online 2 February 2024

Keywords:
Iridium complex
B-embedded
Near-Infrared
OLED
Phosphorescence

ABSTRACT

Pure near-infrared (NIR) phosphorescent materials with emission peak larger than 700 nm are of great significance for the development of optoelectronics and biomedicine. We have designed and synthesized two new B-embedded pure near-infrared (NIR)-emitting iridium complexes ($Ir(Bpiq)_2acac$ and $Ir(Bpiq)_2dpm$) with peaks greater than 720 nm. More importantly, they exhibit very narrow phosphorescent emission with full width at half maximum (FWHM) of only about 50 nm (0.12 eV), resulting in a high NIR content (>90%) in their spectrum. In view of better optical property and solubility, the complex $Ir(Bpiq)_2dpm$ was used as the emitting layer of a solution-processed OLED device, and achieved good maximum external quantum efficiency (EQE) (2.8%) peaking at 728 nm. This research provides an important strategy for the design of narrowband NIR-emitting phosphorescent iridium complexes and their optoelectronic applications.

Near-infrared (NIR) ($\lambda > 700$ nm) luminescent materials have received more and more attention in recent years due to their widely applications in organic light emitting diodes (OLEDs), optical communication, night-vision technologies and bioimaging, *etc.* [1–5]. It is worth emphasizing that the heavy metal complexes can be used as a class of excellent room temperature phosphorescent materials [6–19], especially the metal iridium complexes are more promising because of their advantages of stable octahedral coordination structure, high exciton utilization, adjustable excitation and emission wavelengths, and suitable phosphorescent lifetime. However, the innovative development of long-wave high-efficiency near-infrared iridium complex luminescent materials still faces great challenge. On the one hand, it is difficult to achieve luminescence with peak wavelength greater than 720 nm through ligand engineering, and on the other hand, it is also difficult to realize efficient and narrowband near-infrared phosphorescence due to the limitation of the band-gap law. At present, for C∧N ligand-based cyclometalated iridium complexes, expanding the π conjugation of the ligands is an effective strategy to lower the excitation energy and achieve long-wave emission. For example, for the classical green complex $Ir(ppy)_2acac$ ($\lambda_{em} = 520$ nm) (Scheme 1, top) [20], by replacing the pyridine unit in its C∧N ligand with the isoquinoline unit, the emission wavelength of the newly obtained complex $Ir(piq)_2acac$ is redshifted to 622 nm with a redshift of 106 nm [21]. On this basis, the benzene ring unit in the ligand is replaced by the electron-rich benzothiophene unit, and the emission wavelength can be further regulated to 710 nm [22]. Nevertheless, these previously reported NIR iridium complexes tend to exhibit broadband emissions with large full width at half maximum (FWHM > 70 nm), and result in a significant visible light component in the spectrum, which is not conducive to prepare high-performance night vision devices. Therefore, it is of great significance to obtain pure NIR luminescent materials with narrow band emission.

Notably, boron-containing π-conjugated polycyclic units have been widely used in pure organic thermal activation-delayed fluorescence (TADF) materials in recent years because of their special electronic effects and high rigidity, and often can obtain very narrow band emission due to multiple-resonance (MR) effect [23–32]. Moreover, such boron-containing units can also induce a significant spectral redshift effect in metal complex systems [33–35]. For instance, by replacing the benzene ring in the C∧N ligand with a B-embedded dioxygen-bridge unit, the iridium complex can change its emission color from green ($\lambda_{em} = 516$ nm) to deep-red ($\lambda_{em} = 638$ nm) (Scheme 1, top), and also has a narrow band emission (FWHM = 54 nm) [33]. In addition, previous studies have

* Corresponding authors.
E-mail addresses: shichao@just.edu.cn (C. Shi), liqiuxia2019@just.edu.cn (Q. Li), ifeghxie@xmu.edu.cn (G. Xie).

https://doi.org/10.1016/j.cclet.2024.109596
1001-8417/

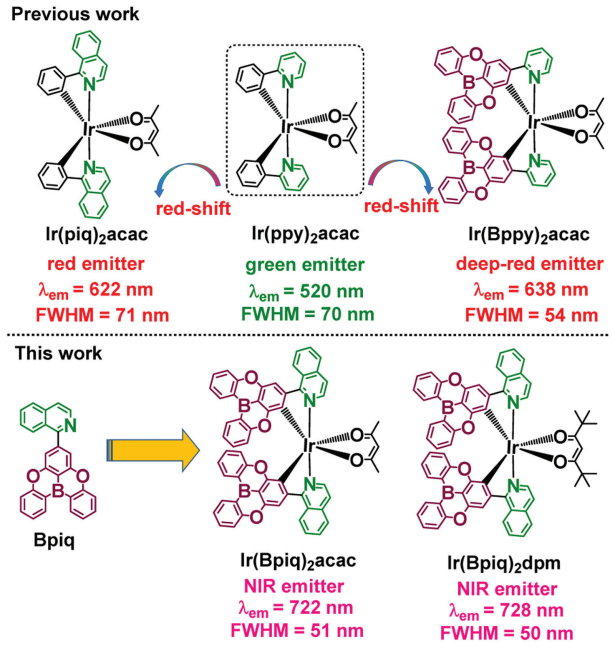

Scheme 1. The structures of (bottom) the NIR-emitting iridium complexes ($Ir(Bpiq)_2acac$ and $Ir(Bpiq)_2dpm$) and (top) previously reported reference complexes ($Ir(piq)_2acac$, $Ir(ppy)_2acac$ and $Ir(Bppy)_2acac$).

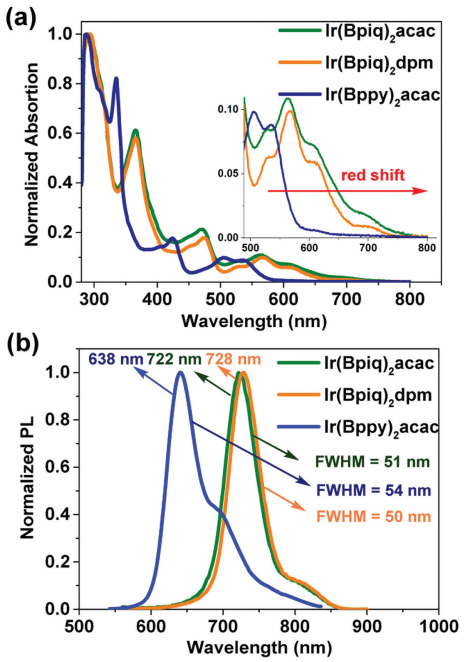

Fig. 1. (a) Absorption and (b) photoluminescence spectra of the NIR-emitting iridium complexes ($Ir(Bpiq)_2acac$ and $Ir(Bpiq)_2dpm$) and the model iridium complex ($Ir(Bppy)_2acac$) in toluene solution (1×10^{-5} mol/L) with an excitation wavelength of 370 nm.

shown that the introduction of different β-diketone ancillary ligands can also fine-tune the luminescence of NIR-emitting iridium complexes [22].

To solve the above problems, we have designed two novel pure NIR phosphorescent iridium(III) complexes ($Ir(Bpiq)_2acac$ and $Ir(Bpiq)_2dpm$) (Scheme 1, bottom), in which the C∧N ligand (Bpiq) contains both the B-embedded dioxygen-bridge unit and the isoquinoline unit, and the β-diketone ancillary ligands are acetylacetone (acac) and 2,2,6,6-tetramethyl-3,5-heptanedione (dpm), respectively. It is found that both complexes exhibit effective near-infrared light with peaks greater than 720 nm and narrow full width at half maximum in toluene ($Ir(Bpiq)_2acac$: $\lambda_{em}=722$ nm, FWHM = 51 nm (0.121 eV), $Ir(Bpiq)_2dpm$: $\lambda_{em}=728$ nm, FWHM = 50 nm (0.116 eV)). In view of better photophysical property and solubility, the NIR-emitting complex $Ir(Bpiq)_2dpm$ was used as the emitting layer of a solution-processed OLED device, and achieved a good maximum external quantum efficiency (EQE) (2.8%) peaking at 728 nm.

The synthetic route of the above B-embedded NIR-emitting complexes is shown in Fig. S1 (Supporting information). First, B-embedded C∧N ligand (Bpiq) can be obtained by the Suzuki coupling reaction using B-embedded dioxygen-bridge unit-based boron ester and 2-chloroisoquinoline. Second, the Bpiq ligand reacts with iridium trichloride to form an iridium chloride bridge intermediate, which then reacts with the auxiliary ligand (acac or dpm) in an alkaline environment to obtain the final product. Next, the structure of both new iridium(III) complexes was completely identified by ^{1}H NMR, ^{13}C NMR, mass spectrometry and elemental analysis..

The photophysical properties of the B-embedded NIR-emitting iridium complexes ($Ir(Bpiq)_2acac$ and $Ir(Bpiq)_2dpm$) and the model iridium complex ($Ir(Bppy)_2acac$) were investigated by spectroscopy (Fig. 1, Table 1, Figs. S2–S4 in Supporting information). According to UV–vis absorption spectra (Fig. 1a and Fig. S2), the strong ligand-centered $\pi\rightarrow\pi^*$ (LC) absorption bands of three complexes is mainly located between 280 nm and 400 nm. For both iridium complexes $Ir(Bpiq)_2acac$ and $Ir(Bpiq)_2dpm$, the lower energy absorption bands, including metal-to-ligand charge transfer (MLCT) and intraligand charge transfer (ILCT), are mainly located in the 450–700 nm range and show a significant redshift compared to the model complex $Ir(Bppy)_2acac$ (Fig. 1a), indicating that the introduction of isoquinoline unit can greatly reduce the excited state energy level. Moreover, due to the fine-tuning of the auxiliary ligand, the absorption band of complex $Ir(Bpiq)_2dpm$ is also slightly redshifted compared to that of complex $Ir(Bpiq)_2acac$ (Fig. 1a). In addition, strong near infrared emissions are observed for both complexes ($Ir(Bpiq)_2acac$: $\lambda_{em}=722$ nm, $Ir(Bpiq)_2dpm$: $\lambda_{em}=728$ nm) in the photoluminescence spectra of toluene solution (Fig. 1b and Table 1). Compared to the model complex ($Ir(Bppy)_2acac$: $\lambda_{em}=638$ nm), their emission peaks show a redshift of nearly 90 nm. In particular,

Table 1
Photophysical properties of the NIR-emitting iridium complexes ($Ir(Bpiq)_2acac$ and $Ir(Bpiq)_2dpm$).

Compound	PL [a,b] (nm)	FWHM[a] (nm)/(eV)	NIR%[c]	$E_{1/2}^{ox}$[d] (V)	E_g[d] (eV)	HOMO/LUMO[d] (eV)	Φ_{PL}	τ[b] (μs)
$Ir(Bpiq)_2acac$	722/718	51/0.121	92	0.09/0.76	1.65	-4.89/-3.24	0.35	2.2
$Ir(Bpiq)_2dpm$	728/724	50/0.116	95	0.03/0.75	1.64	-4.83/-3.19	0.33	2.1

[a] Recorded in toluene (1×10^{-5} mol/L) at 298 K with an excitation wavelength of 370 nm. Φ_{PL} is referred to absolute quantum yields of phosphorescence determined by employing an integrating sphere.
[b] recorded in PS films (1 wt%) (excitation wavelength 370 nm).
[c] Percentage of the NIR component (>690 nm) in the total spectrum.
[d] The HOMO (eV) = $-(E_{onset}^{ox}+4.8)$eV, $E_g=1240/\lambda$, λ is absorption wavelength threshold. LUMO (eV) = E_g + HOMO.

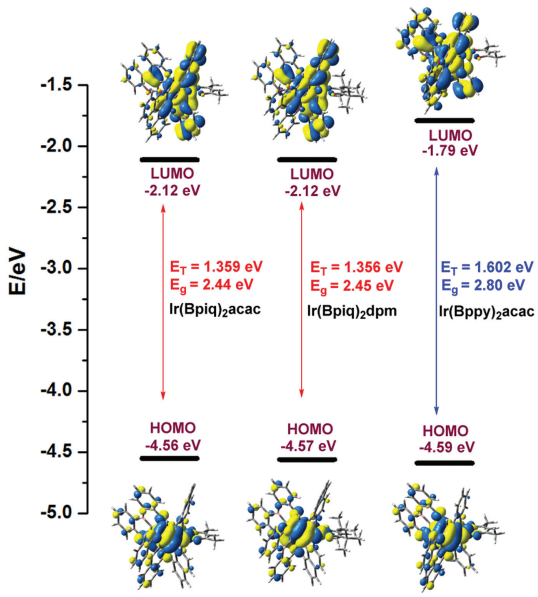

Fig. 2. HOMO and LUMO spatial distribution and energy levels of the NIR-emitting iridium complexes ($Ir(Bpiq)_2acac$ and $Ir(Bpiq)_2dpm$) and the model iridium complex ($Ir(Bppy)_2acac$).

the two NIR emitters ($Ir(Bpiq)_2acac$: FWHM = 51 nm (0.121 eV), $Ir(Bpiq)_2dpm$: FWHM = 50 nm (0.116 eV)) exhibit narrower phosphorescence emission than the model complex (FWHM = 54 nm (0.161 eV)) (Fig. 1b and Table 1), resulting in a high NIR content in their spectrum (NIR% : 92% for $Ir(Bpiq)_2acac$, 95% for $Ir(Bpiq)_2dpm$) (Table 1). Furthermore, their polystyrene (PS) film (1 wt%) also display effective NIR phosphorescence emission ($Ir(Bpiq)_2acac$: $\lambda_{em} = 718$ nm, $\Phi_{PL} = 35\%$, $Ir(Bpiq)_2dpm$: $\lambda_{em} = 724$ nm, $\Phi_{PL} = 33\%$) (Fig. S3a and Table 1). Additionally, the excited state lifetime of the two complexes ($Ir(Bpiq)_2acac$: $\tau = 2.2$ μs, $Ir(Bpiq)_2dpm$: $\tau = 2.1$ μs) is significantly lower than that of the model complex ($Ir(Bpiq)_2dpm$: $\tau = 6.0$ μs) (Fig. S3b and Table 1). In general, the radiative rate constants (k_r) of the two complexes are high and identical (Table S2 in Supporting information). Additionally, the UV–vis and PL spectra of $Ir(Bpiq)_2acac$ and $Ir(Bpiq)_2dpm$ in different solvents showed that the two complexes had a weak solvation effect and the maximum redshift distance is 10 nm (Fig. S4). The Mataga–Lippert plots diagram shows a piecewise linear relationship (Fig. S4e), which is different from the linear relationship of most D-A organic molecules, possibly due to the weak multiple CT states (MLCT and ILCT).

In addition, reversible oxidation behaviors of two complexes are observed in the cyclic voltammetry (CV) (Fig. S5 in Supporting information and Table 1). They all exhibit two oxidation potential peaks (0.02 and 0.76 V for $Ir(Bpiq)_2acac$, 0.09 and 0.78 V for $Ir(Bpiq)_2dpm$), which are attributed to the B-embedded π-conjugation unit and the metal iridium center. As a result, the highest occupied molecular orbital (HOMO) energy levels of $Ir(Bpiq)_2acac$ and $Ir(Bpiq)_2dpm$ are deduced to be 4.82 and 4.89 eV, respectively, while the lowest unoccupied molecular orbital (LUMO) energy levels are 3.17 and 3.25 eV, respectively. Thermogravimetric analysis (TGA) shows that two compounds have good thermal stability with high decom-position temperatures (248 °C for $Ir(Bpiq)_2acac$, 240 °C for $Ir(Bpiq)_2dpm$) (Fig. S6 in Supporting information).

To elucidate the excited state and optical properties of the NIR-emitting iridium complexes ($Ir(Bpiq)_2acac$ and $Ir(Bpiq)_2dpm$) and the model iridium complex ($Ir(Bppy)_2acac$), including the functions of the B-embedded C^N ligand and auxiliary ligand, quantum chemical calculations were performed at the B3LYP/6–31G(d) level (Fig. 2, Figs. S7–S9 and Table S3 in Supporting information). The lowest singlet (S_1) and triplet (T_1) excited states of above three complexes are both dominated by the HOMO → LUMO transition (Table S3). Their HOMOs are mainly distributed on the iridium center, phenyl ring and two oxygen atoms of the B-embedded dioxygen-bridge unit, and a little on the oxygen atoms of the auxiliary ligand (Fig. 2 and Fig. S9), while their LUMOs are mainly located at the isoquinoline unit, phenyl ring and boron atom of the C^N ligand and part of the metal iridium center. As a result, their excited state transitions mainly come from MLCT and ILCT (Table S3). In addition, calculate T_1 energy and band gap (E_g) of the NIR-emitting iridium complexes ($Ir(Bpiq)_2acac$: $E_T = 1.359$ eV, $E_g = 2.44$ eV) and ($Ir(Bpiq)_2dpm$: $E_T = 1.356$ eV, $E_g = 2.45$ eV) are significantly lower than those of the model complex ($Ir(Bppy)_2acac$:

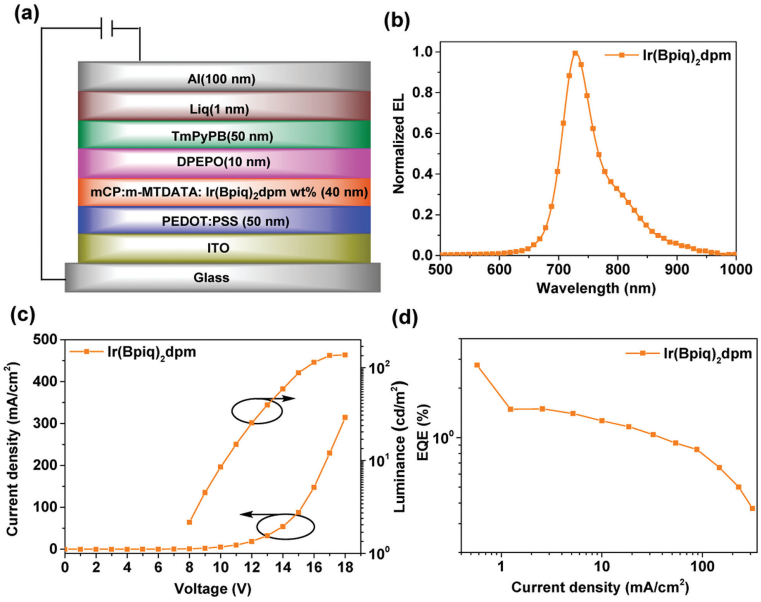

Fig. 3. (a) Configuration of the OLED with dopant $Ir(Bpiq)_2dpm$. (b) EL spectra, (c) current density-voltage-luminance (J–V–L) characteristics and (d) external quantum efficiency (EQE) versus current density relationship for devices of $Ir(Bpiq)_2dpm$.

$E_T = 1.602$ eV, $E_g = 2.80$ eV) (Fig. 2), which explains the fact that the emission wavelength of the NIR-emitting complexes in the experiment is obviously redshifted relative to that of the model complex. Furthermore, the calculated UV spectra are consistent with their experimental UV spectra (Fig. S8).

Additionally, both the calculated dipole moments of the ground state and the excited state indicate that the polarity of $Ir(Bpiq)_2acac$ (4.1554 D for S_0, 3.8422 D for T_1) and $Ir(Bppy)_2acac$ (4.1232 D for S_0, 3.8408 D for T_1) is similar (Figs. S7 and S9), but both are significantly greater than that of $Ir(Bpiq)_2dpm$ (3.7604 D for S_0, 3.4313 D for T_1), suggesting that the changes in auxiliary ligand has a large effect on the polarity of the iridium complex.

In view of better optical property and solubility of the NIR-emitting iridium complex $Ir(Bpiq)_2dpm$ than $Ir(Bpiq)_2acac$, we choose it as the emitter for solution-processed OLED and evaluate its electroluminescence properties (Fig. 3, Table S4, Figs. S10 and S11 in Supporting information). Fig. 3a displays a simple device architecture of the dopant ($Ir(Bpiq)_2dpm$) as follows: ITO/PEDOT:PSS (35 nm)/mCP (49%):m-MTDATA (49%):Ir complex (2%) (40 nm)/DPEPO (10 nm)/TmPyPB (50 nm)/Liq (1 nm)/Al (100 nm), in which ITO is indium–tin oxide, PEDOT is poly(3,4-ethylenedioxythiophene), PSS is poly(styrenesulfonate), mCP is 1,3-bis(*N*-carbazolyl)benzene, m-MTDATA is 4,4′,4′′-tris[(3-methylphenyl)phenylamino]triphenylamine, DPEPO is bis[2-(diphenylphosphino)phenyl]ether oxide, TmPyPB is 1,3,5-tris(3-pyridyl-3-phenyl)benzene, Liq is (8-quinolinolato)lithium. Both mCP and m-MTDATA are used as the mixed host materials because of the balanced carrier transport. PEDOT:PSS is the hole transport material. DPEPO and TmPyPB are electron transport materials. The optimized device at a doping concentration of 5 wt% shows an efficient narrowband NIR emission peak at 728 nm generated only by $Ir(Bpiq)_2dpm$ (Fig. S10 and Table S4), indicating good energy transfer from hosts to the dopant. Notably, it also exhibits a good maximum external quantum efficiencies (EQE) (2.8%), which is comparable to previously reported results for other iridium-containing NIR devices with emission wavelengths less than 720 nm [29].

In summary, two novel B-embedded pure NIR-emitting (>720nm) iridium complexes have been designed and synthesized. They exhibit very narrow phosphorescent emission with FWHM of only about 50 nm (0.12 eV), resulting in a high NIR content (>90%) in their spectrum. Considering better photophysical property and solubility, the complex $Ir(Bpiq)_2dpm$ was used as the emitting layer of a solution-processed OLED device, and achieved good maximum EQE (2.8%) peaking at 728 nm. This research provides an important strategy for the design of narrowband NIR-emitting phosphorescent iridium complexes and their optoelectronic applications.

Declaration of competing interest

The authors declare that they have no known competing financial interests or personal relationships that could have appeared to influence the work reported in this paper.

Acknowledgments

We thanks for financial support from the National Natural Science Foundation of China (Nos. 22171109, 52373195 and 22001097), Natural Science Foundation of Jiangsu Province of China (No. BK20201003), the Postdoctoral Research Foundation of China (No. 2021M701657) and the Opening Project of Key Laboratory of Optoelectronic Chemical Materials and Devices, Ministry of Education, Jianghan University (No. JDGD-202301).

Supplementary materials

Supplementary material associated with this article can be found, in the online version, at doi:10.1016/j.cclet.2024.109596.

References

[1] C. Li, Y. Pang, Y. Xu, et al., Chem. Soc. Rev. 52 (2023) 4392–4442.
[2] H. Li, Y. Kim, H. Jung, J.Y. Hyun, I. Shin, Chem. Soc. Rev. 51 (2022) 8957–9008.
[3] X. Yang, S. Xu, Y. Zhang, et al., Angew. Chem. Int. Ed. 62 (2023) e202309739.
[4] M. Vasilopoulou, A. Fakharuddin, F.P.G.D. Arquer, et al., Nat. Photonics 15 (2021) 656–669.
[5] A. Minotto, P.A. Haigh, Ł.G. Łukasiewicz, et al., Light Sci. Appl. 9 (2020) 70–80.
[6] M.A. Baldo, M.E. Thompson, S.R. Forrest, Nature 403 (2000) 750–753.
[7] J. Zhou, J. Li, K.Y. Zhang, S. Liu, Q. Zhao, Coordin. Chem. Rev. 453 (2022) 214334.
[8] R. Zeng, N. Li, F. Li, et al., Inorg. Chem. Front. 10 (2023) 3263–3272.
[9] G. Lu, Z.G. Wu, R. Wu, et al., Adv. Funct. Mater. 31 (2021) 2102898.
[10] C. Shi, H. Huang, Q. Li, et al., Adv. Optical. Mater. 9 (2021) 2002060.
[11] H.Y. Park, A. Maheshwaran, C.K. Moon, et al., Adv. Mater. 32 (2020) 2002120.
[12] G. Li. N. Li, Y. Cao, et al., Inorg. Chem. 61 (2022) 10548–10556.
[13] M. Penconi, A.B. Kajjam, M.C. Jung, et al., Chem. Mater. 34 (2022) 574–583.
[14] Q. Li, C. Shi, M. Huang, et al., Inorg. Chem. 60 (2021) 17699–17704.
[15] Q. Li. C. Shi, M. Huang, et al., Dalton. Trans. 50 (2021) 16304–16310.
[16] S. Jia. W. Wang, S. Qin, et al., Chin. Chem. Lett. 34 (2023) 107517.
[17] X. Cao. H. Lan, Z. Li, et al., Phys. Chem. Chem. Phys. 17 (2015) 32297–32303.
[18] X. Cao, N. Zhao, G. Zou, et al., Soft. Matter. 13 (2017) 3802–3811.
[19] M. Li, Y. Li, X. Li, et al., Chin. J. Chem. 41 (2023) 1431–1436.
[20] Y. Cao, J. Song, G. Li, et al., ChemistrySelect 6 (2021) 1777–1781.
[21] Y.J. Su, H.L. Huang, C.L. Li, et al., Adv. Mater. 15 (2003) 884–888.
[22] S. Kesarkar, W. Mrýz, M. Penconi, et al., Angew. Chem. Int. Ed. 55 (2016) 2714–2718.
[23] T. Hatakeyama, K. Shiren, K. Nakajima, et al., Adv. Mater. 28 (2016) 2777–2781.
[24] X. Lv, J. Miao, M. Liu, et al., Angew. Chem. Int. Ed. 61 (2022) e202201588.
[25] F. Chen, L. Zhao, X. Wang, et al., Sci. China. Chem. 64 (2021) 547–551.
[26] K. Ye, G. Li, F. Li, et al., Phys. Chem. Chem. Phys. 26 (2024) 2395–2401.
[27] Y. Zhang, G. Li, L. Wang, et al., Angew. Chem. Int. Ed. 61 (2022) e202202380.
[28] Y.X. Hu, J. Miao, T. Hua, et al., Nat. Photonics 16 (2022) 803–810.
[29] X.F. Luo, S.Q. Song, H.X. Ni, et al., Angew. Chem. Int. Ed. 61 (2022) e202209984.
[30] Z. Huang, H. Xie, J. Miao, et al., J. Am. Chem. Soc. 145 (2023) 12550–12560.
[31] F. Zhang, G. Li, C. Shi, et al., Dyes. Pigments 222 (2024) 111902.
[32] G. Li, X. Liu, M. Wu, et al., Dyes. Pigments 208 (2022) 110805.
[33] Q. Li, C. Shi, M. Huang, et al., Chem. Sci. 10 (2019) 3257–3263.
[34] C. Shi, F. Li, Q. Li, et al., Inorg. Chem. 60 (2021) 525–534.
[35] M. Wu, N. Li, C. Shi, et al., Inorg. Chem. Front. 10 (2023) 1262–1269.